

New apparatus for the measurement of the self-discharge of the nickel hydroxide electrode

August Winsel* and Christian Fischer

Gesamthochschule Kassel, D-3500 Kassel (F.R.G.) and VARTA Research & Development Centre, D-6233 Kelkheim/Ts. (F.R.G.)

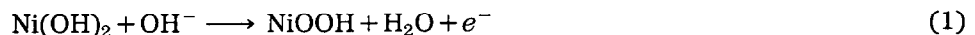
(Received October 20, 1990)

Abstract

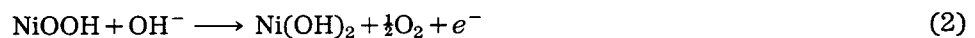
In this report a new method of measurement and equipment [1, 2] are described, that allow easy determination of the activation energy value of the self-decomposition process of the charged Ni(OH)₂/NiOOH electrode. A theoretical description of the method is given and its experimental practicability is demonstrated in addition to preliminary results obtained on differently doped nickel hydroxide samples.

Introduction

One important property which determines the quality of an Ni/Cd accumulator is the rate of self-discharge occurring after the accumulator has been charged. This effect mainly depends on the thermally-activated reduction of the NiOOH in the positive electrode, formed during the charging process according to eqn. (1):



The decomposition of the nickel(III) to nickel(II) illustrated in eqn. (2) leads to oxygen evolution:



Therefore, information on the rate of self-discharge of an NiOOH/Ni(OH)₂ electrode may be obtained by determining the oxygen evolution (depending upon temperature, T , and time, t) from the electrode. The results allow an Arrhenius plot, eqn. (3) to be derived, which will give a value for the molar energy of activation, E_A , of the process.

$$k_n = k_0 \exp\left(-\frac{E_A}{RT}\right) \quad (3)$$

Experimental equipment

The charged nickel hydroxide sample is placed in a container (see Fig. 1), whose heating (and cooling) is controlled by a thermostat; this guarantees

*Author to whom correspondence should be addressed.

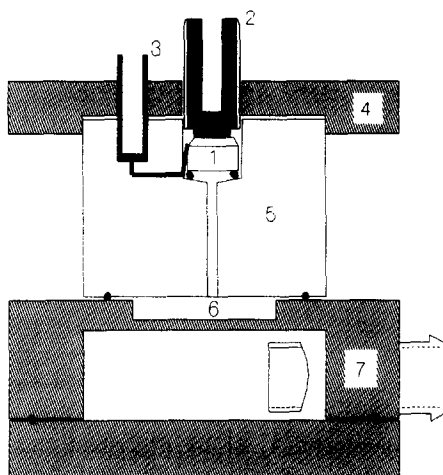


Fig. 1. Details of the equipment used to measure self-discharge. 1, Zinc/oxygen cell; 2, negative contact; 3, positive contact; 4, cover plate (V2A); 5, battery case; 6, sample; 7, tempered container; ■, gaskets.

a quick transmission of heat to the sample. The mould is covered by an element which contains a zinc/oxygen cell; it is made from plexiglas in order to keep the cell at constant temperature. The function of the cell is to determine the amount of oxygen which is evolved during the decomposition of the NiOOH. To achieve stable working conditions, the cell is held, with the aid of a Zener diode, at an operating voltage of 0.7 V. The current of the zinc/oxygen cell, the temperature of the container (which is equivalent to the temperature of the sample), and the time of the experiment are recorded by computer.

Theoretical

The relation between the amount of oxygen (m), which is developed by the self-decomposition of the NiOOH, and the resulting current I of the zinc/oxygen cell can be calculated as follows:

The change, dn/dt , in the amount of oxygen with time is determined by the generated oxygen, which is decreased by the consumption of the zinc/oxygen cell:

$$dn/dt = dm/dt - I/4F \quad (4)$$

The differentiation of the equation for ideal gases ($V = \text{const.}$) in addition to eqn. (4) leads to:

$$\frac{dm}{dt} = \frac{V}{RT} \frac{dp}{dt} + \frac{pV}{R} \frac{d(1/T)}{dt} + \frac{I}{4F} \quad (5)$$

Since the zinc/oxygen cell is kept at (constant) room temperature (plexiglas containment), the current is entirely dependent on the partial pressure, p , of the oxygen. If we consider that diffusion of oxygen into the cell limits the transportation rate, the current will be proportional to the pressure:

$$I = \alpha p \quad (6)$$

The substitution of $p = I/\alpha$ in eqn. (5) results in a formula for the calculation, from the values of the current attained by the zinc/oxygen cell, of the amount of oxygen released by the NiOOH disintegration process:

$$\frac{dm(t)}{dt} = \left[\frac{1}{4F} + \frac{V}{\alpha R} \frac{d(1/T)}{dt} \right] I(t) + \frac{V}{\alpha RT} \frac{dI(t)}{dt} \quad (7)$$

Special cases

(i) *Constant temperature, no sample*

With these assumptions ($d(1/T) = 0$, $dm/dt = 0$) eqn. (7) becomes:

$$\frac{dI(t)}{dt} + \frac{\alpha RT}{4FV} I(t) = 0 \quad (8)$$

Solving this differential equation yields:

$$I(t) = I_0 \exp\left(-\frac{t}{\tau}\right), \quad \tau = \frac{4FV}{\alpha RT} \quad (9)$$

(ii) *Linearly increased temperature $T = T_0 (1 + \beta t)$, no sample*

Two possibilities must be taken into consideration:

(a) The zinc/oxygen cell current is only dependent on the ratio of the partial pressure of oxygen to the total pressure p/p_G , because it is determined by the diffusion, which is independent of the total pressure. Due to the independence of p/p_G and the temperature, this situation can be described in the same way as in (i).

(b) The current depends on the pressure p . Equation (7) changes to:

$$\frac{dI(t)}{dt} + \left(\frac{\alpha RT_0(1 + \beta t)}{4FV} - \frac{T_0(1 + \beta t)d(1/T)}{dt} \right) I(t) = 0 \quad (10)$$

If we neglect the second term, because $|Td(1/T)/dt|$ is rather small, this case can be illustrated by eqn. (9) in addition to a variable relaxation time τ :

$$\tau = \frac{4FV}{\alpha RT_0} \frac{1}{(1 + \beta t)} \quad (11)$$

(iii) *Self-decomposition of the sample by thermal activation with time – proportional increase of temperature $T = T_0 (1 + \beta t)$*

We assumed the oxygen evolution of the sample to be:

$$\frac{dm}{dt} = m_0 \exp\left(-\frac{Q_A}{RT}\right) = m_0 \exp\left(-\frac{T_A}{T}\right) \quad (12)$$

where Q_A = activation energy, and T_A = activation temperature. Neglecting the term $d(1/T)/dt$ in addition with the development of $1/(1 + \beta t)$ to $1 - \beta t$ ($\beta \ll 1$) leads to the following inhomogeneous differential equation:

$$m_0^* \exp\left(\frac{t}{\tau^*}\right) = \frac{1}{4F} I(t) + \frac{V}{\alpha RT} \frac{dI(t)}{dt} \quad (13)$$

$$m_0^* = m_0 \exp(-T_A/T_0), \quad \tau^* = T_0/\beta T_A$$

With the method of the variation of constants and some additional calculations the result is given by:

$$I(t) = I_0 \exp\left(-\frac{t}{\tau}\right) + 4Fm_0^* \frac{\tau^*}{\tau^* + \tau} \left[\exp\left(-\frac{t}{\tau^*}\right) - \exp\left(-\frac{t}{\tau}\right) \right] \quad (14)$$

Experimental

To verify our theory, and to test the air tightness of the test equipment, the container (in the absence of a sample) was kept at constant temperature and the current of the zinc/oxygen cell was registered. The result of this measurement is shown in Fig. 2.

The theoretical curve is shown in addition to the experimental values. To obtain this fit of the two curves, it was necessary to change eqn. (9) to:

$$I(t) = I_0 \exp[-(t - t_{O_2})/\tau] \quad (15)$$

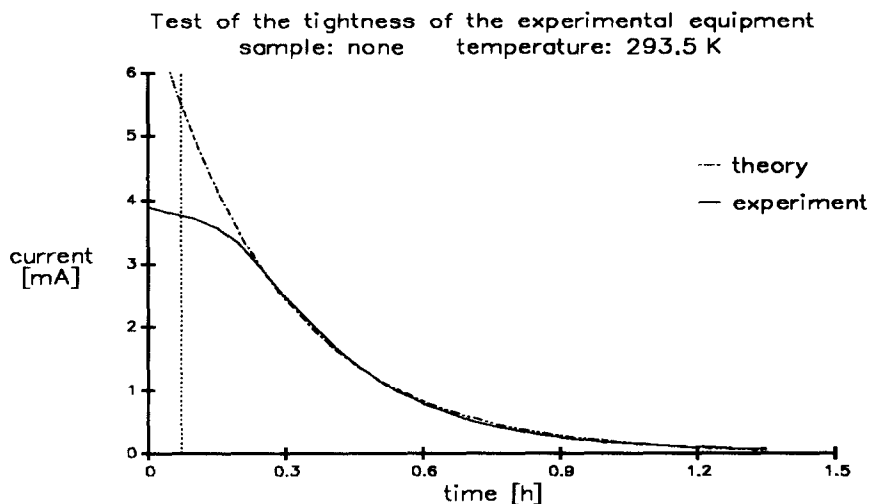


Fig. 2. I/t -characteristic of the zinc/oxygen cell when consuming oxygen.

The correction to time, t_{O_2} (dotted line in Fig. 2), is necessary because of the 'non-ideal-behaviour' of the cell, which is determined by the lower maximum current (limited by the diffusion of oxygen into the cell) and the additional oxygen capacity which is stored in the cell and must be consumed first.

The integration of the curve in the range $t=t_{O_2}$ to $t=\infty$ yields a value for the trough volume of 1.53 cm^3 , which corresponds to the geometrical value of 1.60 cm^3 , indicating the tightness of the equipment and the agreement between theory and experiment. Experimental verification of case (ii) led to analogous results.

Figure 3 shows a typical experimental current-time curve obtained from a so-called 'siderophilic nickel hydroxide' sample, developed by Glemser and Buss of the University of Göttingen, to obtain a substance which was immune to the poisoning effect of iron on the positive electrode in Ni/Fe accumulators [3].

The experiment consists of three different phases. In the first phase the sample is cooled to 0°C , so that its self-decomposition is reduced to very small values. When the residual oxygen is consumed by the zinc/oxygen cell, indicated by a current value smaller than 0.5 mA , the main measurement starts with a proportional increase of temperature with time up to 80°C (phase 2). In phase 3 the temperature is kept constant until the current falls to small values. As can be seen from Fig. 3 sample self-decomposition begins in phase 2 at about 40°C , increasing quickly. In phase 3 the oxygen development rate decreases due to the decreasing amount of available oxidised NiOOH.

In addition to the experimentally determined current of the zinc/oxygen cell, the values for the developed oxygen, calculated from eqn. (12) neglecting the $d(1/T)/dt$ -term, are given in Fig. 3. It is obvious that the two curves have a similar profile; it is therefore possible to determine the molar

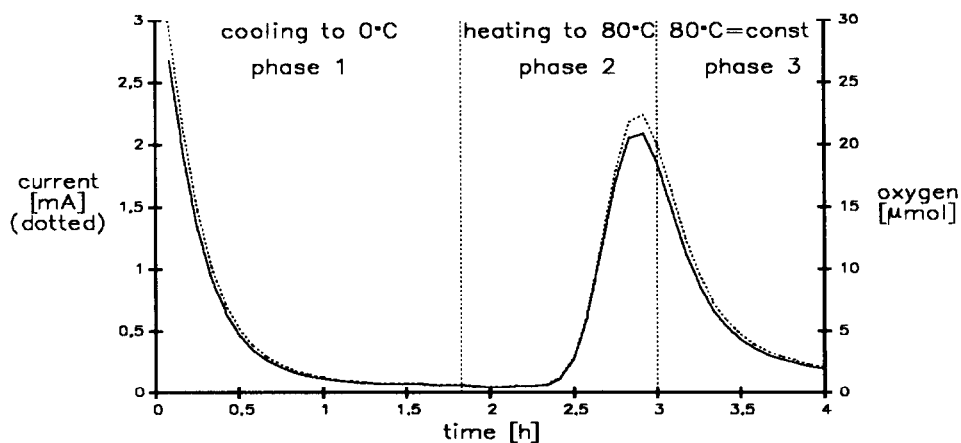


Fig. 3. Calculation of the oxygen developed from the experimentally determined current values: sample siderophilic nickel hydroxide.

energy of activation directly from the current values of phase 2 without calculating the oxygen values (resulting in a maximum failure of only $\pm 2\%$). This is done by an Arrhenius plot, as described above, using the values of phase 2 that belong to the region with increasing values for evolved oxygen.

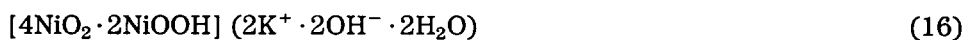
The integration of the curve (phases 2+3) gives the total amount of developed oxygen corresponding to the capacity of the self-discharge of the investigated sample.

Results

Investigations of different $\text{Ni}(\text{OH})_2$ samples doped with K^+ , Li^+ , Fe, Al, and Co resulted in molar energy of activation values (MEA) between 55 and 98 kJ mol^{-1} .

The highest MEA values were achieved by samples with pure KOH- and pure LiOH-doping; values for samples with a mixture of both dopants decreased with increasing amounts of LiOH, and vice versa (see Fig. 4). This effect can be explained by the different manner in which potassium and lithium can be incorporated into the crystal lattice of the nickel hydroxide body.

The potassium ion is built into the highly oxidised gamma-phase of the nickel hydroxide [4, 5]. The phase obtained can be described as follows:



The lattice constant c_0 is enlarged from 0.46 nm ($\beta\text{-Ni}(\text{OH})_2$) to 0.7 nm, and the nickel has an oxidation state of $\text{NiO}_{1.83}$.

According to Dennstedt [6], the incorporation of lithium into the nickel hydroxide lattice can be illustrated by the following reaction mechanism:

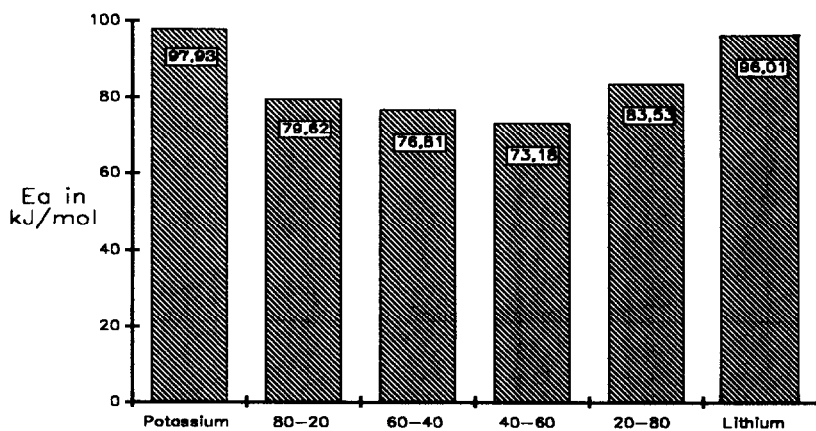
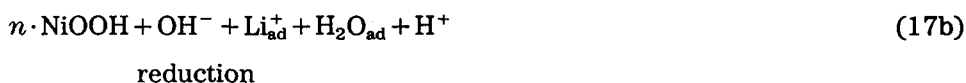


Fig. 4. MEAs for nickel hydroxide doped with K^+ and Li^+ .



During the oxidation of $\beta\text{-Ni}(\text{OH})_2$ to $\beta\text{-NiOOH}$ a transfer of the hydroxide groups within the plane of the crystallographic a axis occurs, leading to the formation of vacancies in the crystal. These vacancies can be occupied by the hydroxide group of an adsorbed lithium hydroxide molecule, while the lithium ion remains in an interstitial position. By analogy, further additional vacancies preferred by hydroxide groups or water molecules are established during the reduction. If there is a coextensive movement of neighbouring hydroxide groups enclosing a layer of nickel atoms, a nickel atom will follow this transfer, resulting in a nickel vacancy which can be taken up by a lithium ion. To sum up, it can be said that the vacancies for two hydroxide ions and one nickel atom formed in the hydroxide and nickel layer of the lattice, can be filled by a hydrated lithium hydroxide molecule ($\text{LiOH} \cdot \text{H}_2\text{O}$) possessing comparable spatial dimensions.

During the formation of the nickel hydroxide in a potassium hydroxide and lithium hydroxide mixture, a two-dimensional expansion of the lattice due to the different incorporation mechanisms of lithium and potassium will take place. This results in an increased lattice energy, corresponding to a decreased MEA for the self-discharge.

Doping of the nickel hydroxide with cobalt and aluminium resulted in decreased activation molar energies of approx. 44–34%, compared with samples doped with pure lithium hydroxide and pure potassium hydroxide. These values might be the result of enlarging the crystal body lattice due to incompatibility of the atomic radius of the dopant. In addition to these values, the MEA from the iron-doped nickel hydroxide ('siderophilic nickel hydroxide') is displayed in Fig. 5. This sample showed a 17% lower value for the MEA of 81 kJ mol^{-1} in comparison with the highest value of 98 kJ mol^{-1} . However, it is in the same range as the values obtained for nickel hydroxide treated with a mixture of potassium hydroxide and lithium hydroxide. Therefore, doping with iron to protect nickel hydroxide from poisoning by iron – occurring in, e.g., Ni/Fe-accumulators – does not greatly increase the self-discharge.

List of symbols

- E_A Molar energy of activation (kJ/mol)
 F Faraday's constant (96487 A s/mol)
 I Current of the zinc/oxygen cell (A)

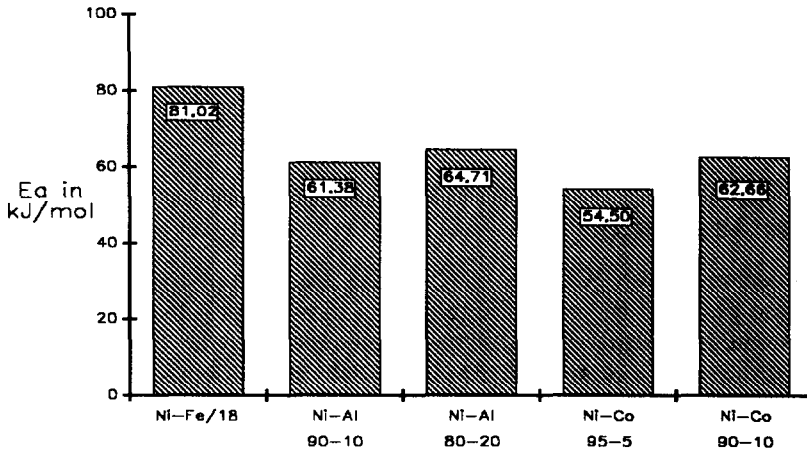


Fig. 5. MEAs of differently doped nickel hydroxide samples.

- k_n Velocity constant (1/s)
 m Amount of oxygen developed by the self-decomposition of the NiOOH (mol)
 n Total amount of oxygen (mol)
 p Partial pressure of oxygen (Pa)
 p_G Total pressure (Pa)
 R Gas constant (8.3143 J/K mol)
 T Absolute temperature (K)
 T_A Temperature of activation (K)
 T_0 Starting value of temperature (K)
 t Time (s)
 t_{O_2} Correction of time (s)
 V Volume of oxygen (m³)
 α Proportional factor (A/Pa)
 β Proportional factor (1/s)
 τ Relaxation time (s)

References

- 1 C. Fischer, Untersuchungen an dotierten Nickelhydroxid-Proben, Gesamthochschule Kassel, 1987.
- 2 G. Leber, Bau einer Oxidationsapparatur zur Messung der Selbstentladung von Nickelhydroxid – Sinterelektroden, *Gesamthochschule Intern. Rep.*, Kassel, 1984.
- 3 G. Krämer, Zur Eisenvergiftung der positiven Nickelhydroxidelektrode und Massnahmen zur deren Immunisierung, *VARTA R&D-Centre, Intern. Rep., TRK 12/85*, Kelkheim, 1985.
- 4 H. Bode, K. Dehmelt and J. Witte, *Electrochim. Acta*, 11 (1966) 1079–1087.
- 5 H. Bode, K. Dehmelt and J. Witte, *Z. Anorg. Allg. Chem.*, 366 (1969) 1–2.
- 6 W. Dennstedt, Modellvorstellung über Quellung und Kapazität des Nickelhydroxids durch Einbau von Lithiumionen, *VARTA R&D-Centre Intern. Rep. EK 13/86*, Kelkheim, 1986.